labeled FKBP and the ^{15}N-labeled FKBP-FK506 complex suggests that significant changes occur in these loop regions following drug binding. Thus, the distinct inhibitory effects that result from FK506 and rapamycin binding (*8*) may involve their influence on the geometry of these loops.

We have recently provided evidence suggesting that the mechanism of rotamase catalysis is due to noncovalent stabilization of a twisted amide in the transition state of the reaction (*23, 24*), rather than formation of a covalent tetrahedral intermediate. A similar mechanism has been proposed for the rotamase cyclophilin (*25, 26*). All Lys, Ser, and Thr side chains in FKBP are directed away from the active site, and the Cα of Cys^{22} is 11 Å from that of Trp^{59} toward the narrow end of the molecule. The pipecolinyl ring of FK506, which contacts Trp^{59}, probably mimics the proline ring of a natural peptide substrate that is subject to rotamase catalysis. Thus, the aforementioned residues are too far from the active site to add to the peptidyl–prolyl amide carbonyl and facilitate rotation about the C–N bond. Site-directed mutagenesis is being used to determine the role of the tyrosines and other key residues found in the active site (Fig. 2D).

Several higher molecular weight FK506- and rapamycin-binding proteins have recently been reported (*27*). The immunophilins of molecular weight 13,000 and 27,000 contain FKBP-like domains of ~110 amino acids that share high sequence identity to FKBP (*28*). Aromatic residues that correspond to Trp^{59}, Tyr^{82}, and Phe^{99}, which line the drug-binding pocket, are conserved in these proteins and in all FKBPs identified from different organisms to date (*8*), suggesting that the ligand-binding pocket is similar in all FKBPs. Thus, the present structure of human FKBP may be relevant to understanding not only its own enzymatic and drug-binding properties, but those of all members of this emerging family of proteins.

Note added in proof: A report has appeared noting the identity of FKBP to inhibitor-2 of protein kinase C (PKCI-2) (*29*); however, we find that FKBP does not inhibit the kinase activity of isolated protein kinase C or protein kinase C–mediated events in cells (*32*).

REFERENCES AND NOTES

1. M. W. Harding *et al.*, *Nature* **341**, 758 (1989).
2. J. J. Siekierka *et al.*, *ibid.*, p. 755.
3. B. E. Bierer *et al.*, *Proc. Natl. Acad. Sci. U.S.A.* **87**, 9231 (1990).
4. R. E. Handschumacher *et al.*, *Science* **226**, 544 (1984).
5. G. Fisher *et al.*, *Nature* **337**, 476 (1989).
6. N. Takahashi, T. Hayano, M. Suzuki, *ibid.*, p. 473.
7. T. Hultsch *et al.*, *Proc. Natl. Acad. Sci. U. S. A.*, in press.
8. S. L. Schreiber, *Science* **251**, 283 (1991).
9. A. T. Brünger and M. Karplus, *Acc. Chem. Res.* **24**, 54 (1991) for review; R. Kaptein, E. R. P. Zuiderweg, R. M. Scheek, R. Boelens, W. F. van Gunsteren, *J. Mol. Biol.* **182**, 179 (1985); A. T. Brünger, G. M. Clore, A. M. Gronenborn, M. Karplus, *Proc. Natl. Acad. Sci. U.S.A.* **83**, 3801 (1986); M. Nilges, G. M. Clore, A. M. Gronenborn, *FEBS Lett.* **229**, 317 (1988); M. Nilges, in *Computational Aspects of the Study of Biological Macromolecules by NMR*, J. C. Hoch, Ed. (Plenum, New York, in press); A. T. Brünger, *X-PLOR Manual, Version 2.1*, (Yale University, New Haven 1990).
10. M. K. Rosen, S. W. Michnick, M. Karplus, S. L. Schreiber, *Biochemistry*, in press.
11. A. Kumar, G. Wagner, R. R. Ernst, K. Wüthrich, *J. Am. Chem. Soc.* **103**, 3654 (1981); M. P. Williamson *et al.*, *J. Mol. Biol.* **182**, 295 (1985).
12. R. F. Standaert, A. Galat, G. L. Verdine, S. L. Schreiber, *Nature* **346**, 671 (1990).
13. T. J. Wandless, S. W. Michnick, M. K. Rosen, M. Karplus, S. L. Schreiber, *J. Am. Chem. Soc.* **113**, 2339 (1991).
14. A. Pardi, M. Billeter, K. Wüthrich, *J. Mol. Biol.* **180**, 741 (1984); D. Neuhaus, G. Wagner, M. Vasak, J. H. R. Kagi, K. Wüthrich, *Eur. J. Biochem.* **151**, 257 (1985); G. Wagner *et al.*, *J. Mol. Biol.* **196**, 611 (1987); E. R. P. Zuiderweg, R. Boelens, R. Kaptein, *Biopolymers* **24**, 601 (1985).
15. J. S. Richardson, *Nature* **268**, 495 (1977).
16. For example, gyceraldehyde phosphate dehydrogenase [D. Moras *et al.*, *J. Biol. Chem.* **250**, 9137 (1975)].
17. C. Chothia, *Annu. Rev. Biochem.* **53**, 537 (1984); Y. N. Chirgadze, *Acta Crystallogr.* **A43**, 405 (1987).
18. O. B. Ptitsyn and A. V. Finkelstein, *Q. Rev. Biophys.* **13**, 339 (1980).
19. G. D. Van Duyne, R. F. Standaert, P. A. Karplus, S. L. Schreiber, J. Clardy, *Science*, **252**, 839 (1991).
20. T. A. Jones, T. Bergfors, J. Sedzik, T. Unge, *EMBO J.* **7**, 1597 (1988).
21. R. Huber *et al.*, *J. Mol. Biol.* **198**, 499 (1987).
22. P. J. Bjorkman *et al.*, *Nature* **329**, 506 (1987); *ibid.*, p. 512.
23. M. K. Rosen, R. F. Standaert, A. Galat, M. Nakatsuka, S. L. Schreiber, *Science* **248**, 863 (1990).
24. M. W. Albers, C. T. Walsh, S. L. Schreiber, *J. Org. Chem.* **55**, 4984 (1990).
25. J. Liu, M. Albers, C. Chen, S. L. Schreiber, C. T. Walsh, *Proc. Natl. Acad. Sci. U.S.A.* **87**, 2304 (1990).
26. R. K. Harrison and R. L. Stein, *Biochemistry* **29**, 1684 (1990).
27. H. Fretz *et al.*, *J. Am. Chem. Soc.* **113**, 1409 (1991).
28. Y.-J. Jin, M. W. Albers, B. E. Bierer, S. L. Schreiber, S. J. Burakoff, *Proc. Natl. Acad. Sci. U. S. A.*, in press. A. Galat, W. S. Lane, R. F. Standaert, S. L. Schreiber, in preparation.
29. M. G. Goebl, *Cell* **64**, 1051 (1991).
30. Starting structures for the simulated annealing protocol consisted of FKBP polypeptide chains with random backbone dihedral angles. The conformational search phase consisted of 20 ps of molecular dynamics at 1000 K under the influence of a force field devised for simulated annealing studies. A quartic repulsion potential was used in the force field in place of the standard CHARMM van der Waals potential for purposes of computational efficiency. The force constant of the repulsive potential (E_{REPEL}) was scaled to 0.002 kcal mol^{-1} $Å^{-4}$ during the conformational search to allow atoms to pass freely through each other. The distance restraint potential target function (E_{NOE}) was a square well with harmonic walls at the upper and lower bounds of the distance restraints and a harmonic plus linear switching function at 0.5 Å above the upper bound. The harmonic force constant was 50 kcal mol^{-1} $Å^{-2}$ and the linear component had a slope of 5 kcal mol^{-1} $Å^{-1}$. The purpose of this phase was to obtain an unbiased search of conformational space with a force field dominated by the experimental target function. The annealing phase consisted of two stages. First, during a 10-ps interval the slope of the linear component of E_{NOE} was increased to 50 kcal mol^{-1} $Å^{-1}$ and the scale of E_{REPEL} was raised to 0.1 kcal mol^{-1} $Å^{-4}$. Second, the distance restraint potential was made harmonic at both the lower and upper distance bounds, experimental dihedral restraints were introduced, the scale of E_{REPEL} was increased to 4.0 kcal mol^{-1} $Å^{-4}$, and the temperature was adjusted from 1000 K to 300 K in steps of 25 K over 2.8 ps. The experimental dihedral potential (E_{cdihe}) was a square well with harmonic walls at the upper and lower bounds with a force constant of 200 kcal mol^{-1} rad^{-2}. The refinement phase consisted of 1000 steps of steepest descent minimization in which the full CHARMM force field including electrostatic and van der Waals nonbonded terms were used (*31*). Statistics were calculated with the program X-PLOR (*9*). Energy analysis was performed with the standard CHARMM force field (*31*).
31. B. R. Brooks *et al.*, *J. Comput. Chem.* **4**, 187 (1983).
32. M. W. Albers *et al.*, *Biomed. Chem. Lett.*, in press.
33. Coordinates of the 21 final structures and of the minimized average structure will be deposited in the Brookhaven Protein Data Bank along with a list of all experimental restraints.

Supported by the National Institute of General Medical Sciences (GM-38627, awarded to S.L.S; GM-30804, awarded to M.K.). National Science Foundation predoctoral fellowships to M.K.R. and T.J.W. are gratefully acknowledged. We thank S. Shambayati for pointing out the novelty of the loop crossing topology in FKBP. NMR spectra were obtained through the auspices of the Harvard University Department of Chemistry Instrumentation Center, which was supported by NIH grant 1-S10-RR04870 and NSF grant CHE 88-14019.

29 January 1991; accepted 1 April 1991

Atomic Structure of FKBP-FK506, an Immunophilin-Immunosuppressant Complex

GREGORY D. VAN DUYNE, ROBERT F. STANDAERT, P. ANDREW KARPLUS, STUART L. SCHREIBER,* JON CLARDY*

The structure of the human FK506 binding protein (FKBP), complexed with the immunosuppressant FK506, has been determined to 1.7 angstroms resolution by x-ray crystallography. The conformation of the protein changes little upon complexation, but the conformation of FK506 is markedly different in the bound and unbound forms. The drug's association with the protein involves five hydrogen bonds, a hydrophobic binding pocket lined with conserved aromatic residues, and an unusual carbonyl binding pocket. The nature of this complex has implications for the mechanism of rotamase catalysis and for the biological actions of FK506 and rapamycin.

IN AN ACCOMPANYING REPORT (*1*), THE function of FKBP (*2, 3*) was discussed, and its structure, determined by nuclear Overhauser effect (NOE)–restrained molecular dynamics, was described. After this structure had been determined, experiments were under-

taken to examine the nature of FKBP-ligand interactions. In this report, we present the atomic structure of the complex formed by human FKBP and FK506 based on a single-crystal x-ray diffraction study to 1.7 Å resolution. The protein component (Fig. 1) is a five-stranded antiparallel β sheet wrapping with a right-handed twist around a short α helix. The five-stranded antiparallel β-sheet framework includes residues 2 to 8, 21 to 30, 35 to 38 with 46 to 49, 71 to 76, and 97 to 106 (*4*) with topology +3, +1, −3, +1 (*5*). The α helix is formed by residues 57 to 63. Thus, the fold of the protein is identical to that independently seen in the solution structure of uncomplexed FKBP (*1*).

FK506 binds in a shallow cavity between the α helix and the β sheet, with roughly 430 $Å^2$ (50%) of the ligand surface being buried at the protein-ligand interface and the remainder, encompassing the region around the allyl and the cyclohexyl groups, being exposed to solvent. Loops composed of residues 39 to 46, 50 to 56, and 82 to 95 flank the binding pocket, which is lined with conserved, aromatic residues. The side chains of Tyr^{26}, Phe^{46}, Phe^{99}, and Val^{55}-Ile^{56} make up the sides of the pocket, while the indole of Trp^{59}, in the α helix, is at the end of the pocket and serves as a platform for the pipecolinyl ring, the most deeply buried part of FK506 (Fig. 2). Both the location and the orientation of the pipecolinyl ring are consistent with NOEs observed between FK506 and Trp^{59}, Phe^{46}, and Tyr^{26} (*6*). As might be expected, there are no water molecules in the hydrophobic binding pocket.

There are five hydrogen bonds between FKBP and FK506: Ile^{56}-NH to C-1 lactone carbonyl, Glu^{54}-CO to C-24 hydroxyl, Gln^{53}-CO to C-24 hydroxyl (through a water molecule), Asp^{37}-CO_2^- to C-10 hemiketal hydroxyl, and Tyr^{82}-OH to C-8 amide oxygen. The first three, involving residues near the NH_2-terminus of the helix, form an array reminiscent of the antiparallel sheet interactions in many peptide-protein (especially protease) complexes, suggesting that the region of FK506 spanning C-24 to C-1 through the lactone linkage may mimic a dipeptide. As has been noted (*7*), the adjacent pyranose-pipecolinyl region also resembles a dipeptide, and thus FK506 may prove to be an illustrative example of extended peptidomimicry. The fifth hydrogen bond, involving the C-8 amide, is the most conspicuous because it is nearly orthogonal to the carbonyl plane and thus may be relevant to the mechanism of rotamase activity.

Protein-protein hydrogen bonds help maintain the organization of the binding pocket, particularly in restraining the flexible loops, which assume well-defined conformations in the complex. For instance, Asp^{37}-CO_2^- forms hydrogen bonds not only with the C-10 hemiketal hydroxyl of FK506, but also with the Arg^{42} and Tyr^{26} side chains (*8*). Two well-ordered water molecules bridge the loop from Tyr^{82} to Ala^{95} by mediating hydrogen bonds from Tyr^{82}-NH to Ala^{95}-CO and from Gly^{83}-CO to Pro^{92}-CO. Three residues within this loop, Tyr^{82}, His^{87}, and Ile^{91}, contact FK506, with the side chains of the latter two forming a surface complementary to the pyranose methyl group region. The observed loop geometry thus plays a major role in ligand binding, but it also forces Ala^{81} to adopt unfavorable ϕ,Ψ values of −141° and −120°, respectively.

The conformation of bound FK506 was determined unambiguously (strong electron density and low thermal parameters). The conformational difference between free and bound FK506 is striking. The molecular geometries of free FK506 as determined by x-ray diffraction (*9, 10*) and of FK506 bound to FKBP are shown in Fig. 3. A provocative finding in view of FKBP's rotamase activity is the nature of the amide bond. In both the bound and unbound forms of FK506, the amide is planar; there is no intimation of partial rotation (no constraints were imposed on the planarity of the amide during refinement of the bound ligand). However, in unbound FK506, the amide bond is cis, while in the complex the bond is trans (Fig. 3, B and D, arrow). A model for FK506's ability to inhibit rotamase activity has focused on the orthogonality of the adjacent carbonyls at C-8 and C-9 (*11*). It was postulated that the keto carbonyl acts as a mimic of the carbonyl in

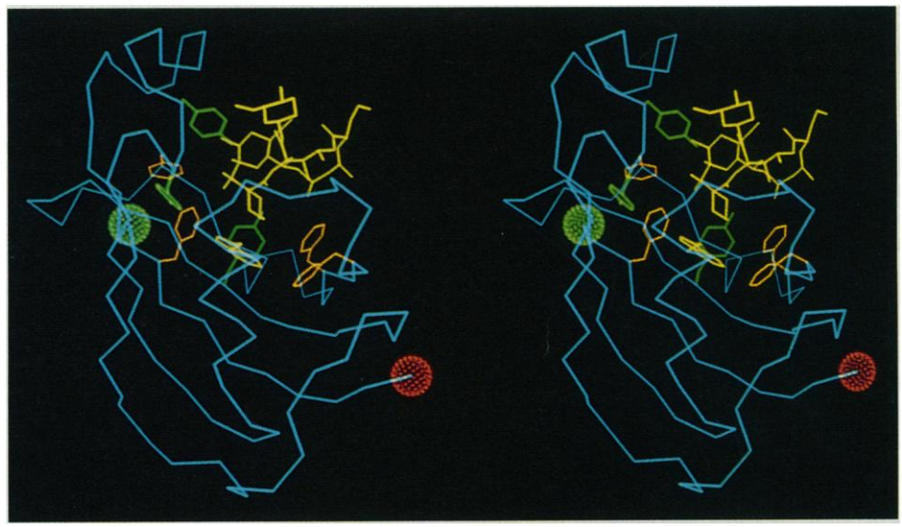

Fig. 1. A stereo view of the FKBP-FK506 complex showing a Cα tracing for the protein (cyan) with bound FK506 (yellow) and aromatic side chains of the binding pocket (Tyr, green; Phe, red-orange; and Trp, yellow); green and red dot surfaces denote the NH_2- and COOH-termini, respectively. The overexpression and purification of recombinant human FKBP have been described (*19*). Crystals of FKBP-FK506 were grown within 1 to 2 weeks at room temperature from 10-μl hanging droplets containing 10 mg/ml protein-FK506 complex, 1.7 M $(NH_4)_2SO_4$, and 0.1 M phosphate, pH 5.9. The crystals are tetragonal, space group $P4_22_12$, with cell constants a = 58.07 ± 0.02 Å, c = 55.65 ± 0.02 Å, and contain one protein-FK506 complex in the asymmetric unit. Data to 1.7 Å [69,770 measurements of 10,855 unique reflections, 99% complete, R_{sym} = 0.0539 (*20*)] were measured from one crystal with dimensions 0.4 mm by 0.4 mm by 0.3 mm with the use of a San Diego Multiwire Systems Mark II detector (*21*) and graphite-monochromated Cu Kα radiation. Experimental phases at 3 Å resolution were obtained by using conventional multiple isomorphous replacement (MIR) techniques with $HgCl_2$ (2 mM), K_2PtCl_4 (2 mM), and Se-Met derivatives. The MIR electron density map allowed the chain to be traced and showed the positions of buried side chains. The availability of a preliminary structure from NMR studies (*1*) greatly facilitated the chain tracing. The initial model was refined first at 3.0 Å and then at 2.6 Å by simulated annealing followed by manual adjustments. Traditional restrained least squares refinement was used at higher resolution. Electron density for the bound FK506 could be seen in the MIR map, but the ligand was not included in the model until electron density maps calculated at higher resolution (2.2 Å) showed its conformation more clearly. The stereochemical restraints used in ligand refinement were restricted to terms for bond lengths, bond angles, and improper dihedral angles (for planar sp^2 carbons and chiral centers). Model building was carried out with the program FREIBAU (*22*), and all of the refinements were carried out with X-PLOR (*23*). The current model, including FKBP, FK506, and 79 water molecules, has an R factor of 0.170 (*20*) for data from 10 to 1.7 Å. The root-mean-square deviations of bond lengths, bond angles, and improper dihedral angles (planarity and chirality) from their ideal values are 0.01 Å, 2.8°, and 1.4°, respectively. All main chain atoms, buried side chain atoms, and ligand atoms are well defined in the final $2F_o - F_c$ electron density map (*20*).

G. D. Van Duyne and J. Clardy, Department of Chemistry, Baker Laboratory, Cornell University, Ithaca, NY 14853–1301.
R. F. Standaert and S. L. Schreiber, Department of Chemistry, Harvard University, Cambridge, MA 02138.
P. A. Karplus, Department of Biochemistry, Molecular and Cell Biology, Cornell University, Ithaca, NY 14853.

*To whom correspondence should be addressed.

a twisted peptidyl-prolyl amide bond. This orthogonality is maintained in the complex. Interestingly, although there are no hydrogen bonds to the C-9 keto oxygen, there are three ε-hydrogens in contact with this atom, one each from the conserved aromatic residues Tyr^{26}, Phe^{36}, and Phe^{99} (Fig. 2). [Aromatic C–H···O stabilizing interactions have been noted previously (*12*).] This carbonyl binding pocket, which resides out of the plane of the amide bond in FK506, might also prove to be relevant to catalysis; a novel form of transition-state stabilization involving C–H···O interactions would then be implicated.

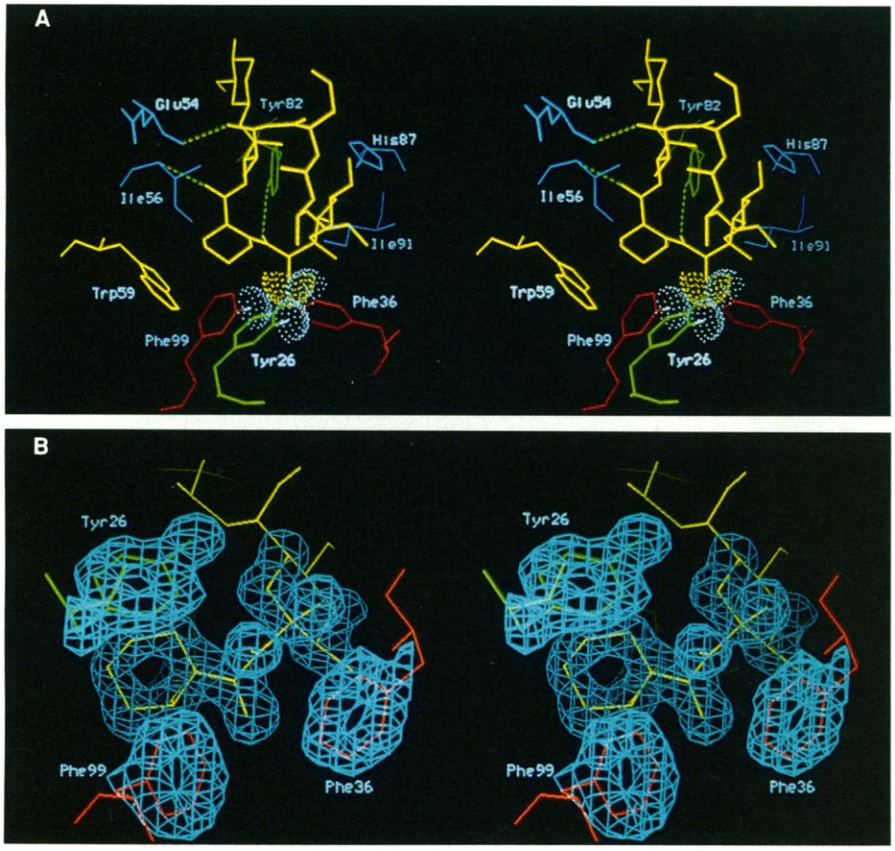

Fig. 2. (**A**) A stereo view of the binding region of FKBP-FK506 showing FK506 (yellow) and selected residues of the hydrophobic binding pocket (Tyr, green; Phe, red-orange; and Trp, yellow). Hydrogen bonds are shown between the C-1 ester carbonyl and the NH of Ile^{56}, the C-24 hydroxyl and the main chain carbonyl of Glu^{54}, and the C-8 amide and the phenolic-OH of Tyr^{82}. The C-9 carbonyl binding pocket is illustrated with van der Waals dot surfaces for the ε-CHs of Tyr^{26}, Phe^{36}, and Phe^{99}. The side chains from residues Tyr^{26}, Phe^{36}, Asp^{37}, Arg^{42}, Phe^{46}, Glu^{54}, Val^{55}, Ile^{56}, Trp^{59}, Tyr^{82}, His^{87}, Ile^{91}, and Phe^{99} are within 4 Å of FK506. (**B**) A stereo view of a selected region of electron density in the binding pocket showing the pipecolinyl ring, the C-8 amide and C-9 keto carbonyls, and the three aromatic residues that make up the C-9 carbonyl binding pocket. The electron density is from a $2F_o - F_c$ map (*20*) calculated at 1.7 Å resolution and contoured at 18% of the maximum value (2σ).

The two conformations also differ in the orientation of the pyranose ring. In the unbound form, the pyranose ring is on the outside of the large macrocycle, while in the bound form it is on the inside, creating a tightly packed hydrophobic region. The orientation of the loop C-15–C-26 also differs in the two forms in that the methoxyl at C-15 is inside the macrocycle in the free form and outside in the complexed form. This methoxyl is brought much closer to the methoxyl on the pyranose ring in the complex, with a water molecule located between them. In both forms the lactone has the expected trans conformation.

These conformational changes have modest energetic consequences—~3 kcal mol^{-1} more steric energy for bound FK506 than for unbound (*13*). Notably, complexed FK506 more closely resembles free rapamycin (*14*) (Fig. 3) than it does free FK506, which suggests that the higher affinity of rapamycin to FKBP [dissociation constant K_d = 0.2 nM for rapamycin versus 0.4 nM for FK506 (*15*)] reflects its greater preorganization. Earlier it had been suggested that FK506 and rapamycin are comprised of common structural elements necessary for binding to FKBP and distinct connecting loops that confer their distinct biological properties (*15*). The x-ray structure reveals that the proposed binding elements of FK506 are contacting FKBP. The similarity in the conformation of this region to the corresponding region in rapamycin (Fig. 3) and the similarity in the pipecolinyl resonances in the nuclear magnetic resonance (NMR) spectra of the two FKBP-drug complexes support a common mode of drug binding. Indeed, these contact elements constitute the predominant structural features of 506BD (*16*), thus suggesting a structural basis for the tight binding of this nonnatural ligand to FKBP.

These investigations provide a structural framework to improve upon the high-affinity interactions of a clinically promising immunosuppressant with its predominant cytosolic receptor in the T cell. The high sequence homology of other members of the FKBP family (*17*)

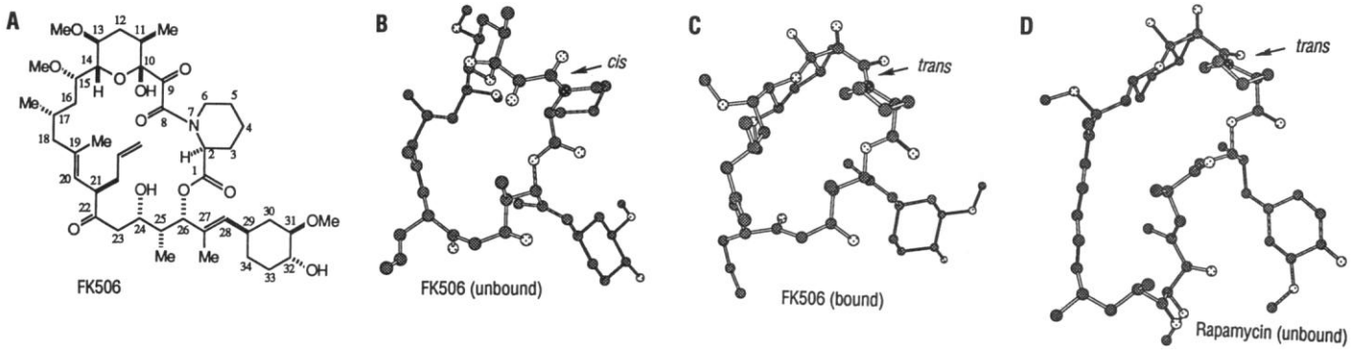

Fig. 3. Structures of FK506 and rapamycin. (**A**) Chemical formula of FK506 with the numbering scheme used in the text and perspective drawings of (**B**) unbound FK506 as determined from x-ray diffraction analysis (7). (**C**) FK506 bound to FKBP, and (**D**) rapamycin as determined from x-ray diffraction analysis (*14*).

suggest that their interactions may be evaluated with use of this structure. A detailed comparison of the structure of FKBP and the FKBP-FK506 complex is likely to provide additional insights into the mechanism of rotamase catalysis. The determination of the molecular interactions of the binary complex reported herein with protein targets implicated in studies of signaling mechanisms could provide profound insights into the biological properties of these molecules (*18*).

REFERENCES AND NOTES

1. S. W. Michnick, M. K. Rosen, T. J. Wandless, M. Karplus, S. L. Schreiber, *Science* **252**, 836 (1991).
2. J. J. Siekierka, S. H. Y. Hung, M. Poe, C. S. Lin, N. H. Sigal, *Nature* **341**, 755 (1989).
3. M. W. Harding, A. Galat, D. E. Uehling, S. L. Schreiber, *ibid.*, p. 758.
4. Surface areas and secondary structure were calculated with the program DSSPNOV [W. Kabsch and C. Sander, *Biopolymers* **22**, 2577 (1983)].
5. J. S. Richardson, *Nature* **268**, 495 (1977).
6. T. J. Wandless, S. W. Michnick, M. K. Rosen, M. Karplus, S. L. Schreiber, *J. Am. Chem. Soc.* **113**, 2339 (1991).
7. M. W. Albers, C. T. Walsh, S. L. Schreiber, *J. Org. Chem.* **55**, 4984 (1990).
8. A. Horovitz, L. Serrano, B. Avron, M. Bycroft, A. R. Fersht, *J. Mol. Biol.* **216**, 1031 (1990).
9. H. Tanaka *et al.*, *J. Am. Chem. Soc.* **109**, 5031 (1987).
10. The solution conformations for both cis and trans rotamers of FK506, suggested by NMR studies, show little similarity to the conformation of bound FK506 [P. Karuso, H. Kessler, D. F. Mierke, *J. Am. Chem. Soc.* **112**, 9434 (1990)].
11. M. K. Rosen, R. F. Standaert, A. Galat, M. Nakatsuka, S. L. Schreiber, *Science* **248**, 863 (1990).
12. K. A. Thomas, G. M. Smith, T. B. Thomas, R. J. Feldmann, *Proc. Natl. Acad. Sci. U.S.A.* **79**, 4843 (1982).
13. Steric energies were computed with the program MacroModel [F. Mohamadi *et al.*, *J. Comput. Chem.* **11**, 440 (1990)].
14. J. A. Findlay and L. Radics, *Can. J. Chem.* **58**, 579 (1980).
15. B. E. Bierer *et al.*, *Proc. Natl. Acad. Sci. U.S.A.* **87**, 9231 (1990).
16. B. E. Bierer, P. K. Somers, T. J. Wandless, S. J. Burakoff, S. L. Schreiber, *Science* **250**, 556 (1990).
17. H. Fretz *et al.*, *J. Am. Chem. Soc.* **113**, 1409 (1991).
18. S. L. Schreiber, *Science* **251** 283 (1991).
19. R. F. Standaert, A. Galat, G. L. Verdine, S. L. Schreiber, *Nature* **346**, 671 (1990).

20. $R_{sym} = \Sigma \mid I - \langle I \rangle \mid / \Sigma I$, R factor $= \Sigma \mid F_o - F_c \mid / \Sigma F_o$, the coefficients of the Fourier sum for a $2F_o - F_c$ electron density map are $(2F_o - F_c)\exp(i\phi_c)$, where I is an observed intensity measured more than once, F_o is an observed structure factor magnitude, and F_c and ϕ_c are the amplitude and phase, respectively, of a structure factor calculated from the refined model.

21. R. Hamlin, *Methods Enzymol.* **114**, 416 (1985); A. J. Howard, C. Nielsen, Ng. H. Xuong, *ibid.*, p. 452.
22. P. A. Karplus, M. J. Daniels, J. R. Herriott, *Science* **251**, 60 (1991).
23. A. T. Brünger, J. Kuriyan, M. Karplus, *ibid.* **235**, 458 (1987).

24. Coordinates of the bound FK506 molecule are available from the authors. The complete refined coordinates of the FKBP-FK506 complex will be deposited in the Brookhaven Protein Data Bank.

Supported by the National Institute of General Medical Sciences (GM-38627, S.L.S.) and by the National Cancer Institute (CA-24487, J.C.). We thank M. Karplus, S. W. Michnick, M. K. Rosen, T. J. Wandless, J. Liu, M. W. Albers, and T. J. Stout for most helpful discussions. The area detector facility was supported by NSF grant DIR-8820910 and crystallographic model building was performed on a graphics workstation donated by Hewlett-Packard.

7 February 1991; accepted 1 April 1991

HBV X Protein Alters the DNA Binding Specificity of CREB and ATF-2 by Protein-Protein Interactions

HUGH F. MAGUIRE, JAMES P. HOEFFLER, ALEEM SIDDIQUI*

The hepatitis B virus (HBV) X gene product trans-activates viral and cellular genes. The X protein (pX) does not bind independently to nucleic acids. The data presented here demonstrate that pX entered into a protein-protein complex with the cellular transcriptional factors CREB and ATF-2 and altered their DNA binding specificities. Although CREB and ATF-2 alone did not bind to the HBV enhancer element, a pX-CREB or pX–ATF-2 complex did bind to the HBV enhancer. Thus, the ability of pX to interact with cellular factors broadened the DNA binding specificity of these regulatory proteins and provides a mechanism for pX to participate in transcriptional regulation. This strategy of altered binding specificity may modify the repertoire of genes that can be regulated by transcriptional factors during viral infection.

CONTROL OF EUKARYOTIC GENE TRANscription is a tightly regulated process mediated by nuclear factors whose availabilities are determined by cell type, differentiation state, and cell cycle (*1*). During viral infection, this system of coordinate regulation is perturbed by the activity of one or more viral gene products. In many cases, these viral proteins activate cellular transcription factors that interact with cis-acting elements present in viral promoters and enhancers, resulting in the expression of viral genes (*1, 2*).

Human HBV infects hepatocytes and causes acute and chronic liver disease. Infection is associated with the development of hepatocellular carcinoma (*3*). The small genome of this virus encodes four genes whose transcriptional activities are controlled by at least four promoters and two enhancer elements (*3, 4*). The 16.5-kD product of the HBV X gene, pX, is a transcriptional trans-activator capable of elevating transcription governed by a variety of viral and cellular control elements (*5, 6*). Similar to the herpes virus VP16 or adenovirus *E1A* gene products (*7, 8*), pX does not bind independently to responsive DNA sequences. An alternative mechanism through which pX might activate gene expression is through protein-protein interactions with cellular transcription factors (*7*).

Several investigators have described transcriptional stimulation of reporter genes linked to the HBV enhancer element that is mediated by pX (*5, 6*). The NF-κB sequence motif within the human immunodeficiency virus long terminal repeat is the target of pX-mediated activation (*6*). A cryptic NF-κB element is located within the HBV enhancer at nucleotide 984. Although a reporter construct containing this HBV sequence is activated tenfold compared to control plasmids (Fig. 1), purified NF-κB does not bind to this sequence motif (*9*). A second pX-responsive element was also localized within the HBV enhancer (Fig. 1). This region contains overlapping binding sites for multiple transcription factors, including NF-1, C/EBP, AP-1, CREB, and ATF (*10*). In

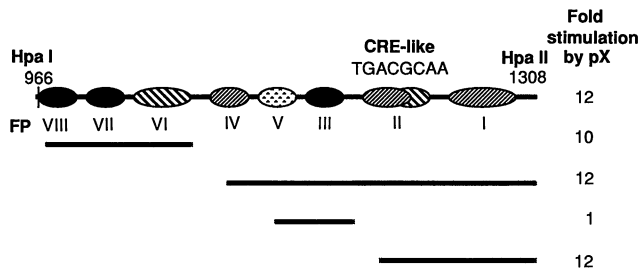

Fig. 1. Elements of the HBV enhancer that are pX-responsive. Luciferase gene expression (*18*) was under the control of the simian virus 40 (SV40) early promoter, which was linked to elements within the HBV enhancer. HepG2 or a stably transformed pX-expressing cell line (GET) was transfected with the HBV enhancer constructs indicated by the black lines, either alone or with a plasmid that encodes pX (*19*). Fold stimulation of transcription in the presence of pX is compared to basal levels achieved with the SV40 early promoter alone. Transfection efficiency was normalized with the pSV2β-galactosidase plasmid. FP, footprint sites protected in the DNase I assay, numbered in the order of their discovery.

H. F. Maguire and A. Siddiqui, Department of Microbiology and Immunology, University of Colorado School of Medicine and Cancer Center, Denver, CO 80262.
J. P. Hoeffler, Division of Medical Oncology, University of Colorado School of Medicine and Cancer Center, Denver, CO 80262.

*To whom correspondence should be addressed.